Quantitative Analysis of Synaptic Contacts Made between Functionally Identified Oralis Neurons and Trigeminal Motoneurons in Cats

Atsushi Yoshida,[1] Hideyuki Fukami,[1] Yoshitaka Nagase,[1] Kwabena Appenteng,[2] Shiho Honma,[1] Li-Fen Zhang,[1] Yong Chul Bae,[3] and Yoshio Shigenaga[1]

[1]Department of Oral Anatomy and Neurobiology, Graduate School of Dentistry, Osaka University, Suita, Osaka 565-0871, Japan, [2]Department of Physiology, University of Ghana Medical School, Accra 2086, Ghana, and [3]Department of Oral Anatomy, Kyungpook University School of Dentistry, Taegu 700-422, Korea

A previous study revealed that rostrodorsomedial oralis (Vo.r) neurons synapsing on trigeminal motoneurons use GABA and/or glycine as neurotransmitters. To determine the number and spatial distribution of contacts, injections of biotinamide and horseradish peroxidase were made into a Vo.r neuron and an α-motoneuron in the jaw-closing (JC) and jaw-opening (JO) motor nucleus, respectively, in 39 cats. All Vo.r neurons responded to low-threshold mechanical stimulation of the oral tissues. Single Vo.r neurons terminating in the JC nucleus (Vo.r-dl neurons; $n = 5$) issued, on average, 10 times more boutons than Vo.r neurons terminating in the JO nucleus (Vo.r-vm neurons; $n = 5$; 4437 vs 445). The Vo.r-dl neuron–JC α-motoneuron pairs ($n = 4$) made contacts on either the soma–dendritic compartment or dendrites, and the Vo.r-vm neuron–JO motoneuron pairs ($n = 2$) made contacts on dendrites, with a range of two to seven contacts. In five of the six pairs, individual or groups of two to three terminals contacted different dendritic branches of a postsynaptic cell. The Vo.r-dl neurons innervated a greater number of counter-stained motoneuronal somata than did the Vo.r-vm neurons (216 vs 26). Total number of contacts per Vo.r neuron was higher for the Vo.r-dl than Vo.r-vm neurons (786 vs 72). The present study demonstrates that axonal branches of Vo.r neurons are divided into two types with different innervation domains on the postsynaptic neuron and that they are highly divergent. The overall effect exerted by these neurons is predicted to be much greater within the JC than JO motoneuron pool.

Key words: trigeminal; contact; sensorineuron; motoneuron; neurobiotin; horseradish peroxidase

Previous studies revealed that the rostrodorsomedial part (Vo.r) of the oral nucleus (Vo) contains a large number of interneurons projecting to either the jaw-closing motor nucleus (Vmo.dl) or the jaw-opening motor nucleus (Vmo.vm) in addition to other brainstem nuclei (Shigenaga et al., 1988a; Olsson and Westberg, 1991; Yoshida et al., 1994; Westberg et al., 1995). Furthermore, the Vo.r is characterized as a region that receives projections mainly from primary afferents innervating the oral and perioral structures (Arvidsson and Gobel, 1981; Shigenaga et al., 1986a,b; Tsuru et al., 1989; Takemura et al., 1991; Moritani et al., 1998) as well as projections from jaw-muscle spindle afferents (Luo and Dessem, 1995; Luo et al., 1995).

Recently, we provided ultrastructural evidence that Vo.r neurons make synaptic contacts on either jaw-closing (JC) or jaw-opening (JO) motoneurons and that all Vo.r premotoneurons that were examined contain pleomorphic vesicles in their terminals contacting the motoneuronal somata or dendrites with symmetric specializations (Shigenaga et al., 2000). In addition, we found that Vo.r-induced monosynaptic IPSP in JC α-motoneurons is suppressed by systemic administration of strychnine or bicuculline, whereas application of both APV and CNQX in the trigeminal motor nucleus (Vmo) unmasks monosynaptic IPSP in JO motoneurons. These results indicate that the Vo.r contains inhibitory interneurons acting directly either on JC or JO α-motoneurons. Further light microscopic (LM) study is essential to determine the net effects produced by the Vo.r neurons on the motoneurons and the spatial distribution patterns of their synaptic sites.

The morphological and physiological properties of synaptic connections made between inhibitory cells and their target postsynaptic cells have been analyzed extensively in the neocortex (Thomson et al., 1996; Tamás et al., 1997) and hippocampus (Buhl et al., 1994; Miles et al., 1996) by using dual intracellular recordings and labeling. In the spinal cord, Fyffe (1991) examined synaptic contacts made by single Renshaw cells on single α-motoneurons and reported that their synapses are restricted to dendrites. Recent spinal cord studies have focused on morphological analyses of the numbers and spatial distribution of group Ia synapses on α-motoneurons (Burke et al., 1979; Brown and Fyffe, 1981; Redman and Walmsley, 1983; Lüscher and Clamann, 1992; Burke and Glenn, 1996) to evaluate conceptual models of the operation of chemical synaptic junctions (Rall et al., 1967; Rall, 1977; Redman, 1979).

In the trigeminal motor system, we offered quantitative morphological data on single jaw-muscle spindle afferent terminations in the Vmo.dl (Shigenaga et al., 1990; Kishimoto et al., 1998) and on their synaptic sites made on single JC α-motoneurons (Yabuta et al., 1996; Yoshida et al., 1999). Com-

Received Dec. 20, 2000; revised May 21, 2001; accepted May 21, 2001.

This work was supported by a grant-in-aid for scientific research from the Ministry of Education, Science and Culture of Japan (11671799) to A.Y. and Y.N. K.A. was supported by a fellowship from the Japan Society for the Promotion of Science. We are grateful to Dr. Michael Dodson for improving the English of the original manuscript.

Correspondence should be addressed to Dr. Yoshio Shigenaga, Department of Oral Anatomy and Neurobiology, Graduate School of Dentistry, Osaka University, 1-8 Yamadaoka, Suita, Osaka 565-0871, Japan. E-mail: sigenaga@dent.osaka-u.ac.jp.

 0270-6474/01/216298-10$15.00/0

parisons of these data with those of second-order sensory premotoneurons are important for determining the morphological principle of synaptic distribution patterns governed by different afferent inputs and for understanding the neural mechanisms underlying motor coordination and masticatory patterns.

Thus, in this study, we analyzed the numbers and spatial distribution of synaptic contacts made by single Vo.r neurons on single JC and JO motoneurons as well as on counter-stained motoneurons.

MATERIALS AND METHODS

Surgical preparations. Experiments were conducted on 39 adult cats in the weight range 2.0–4.2 kg. Anesthesia was initially induced by ketamine (35 mg/kg, i.m.) followed by sodium pentobarbital (40 mg/kg, i.v.), with supplementary doses of sodium pentobarbital (10 mg/ml) being given as necessary to maintain a deep level of anesthesia throughout the experiment. End-tidal $\%CO_2$, electrocardiogram (ECG), and rectal temperature were monitored continuously and maintained within physiological limits, and the depth of anesthesia was monitored frequently by checking the pupil size and pulse rate. All animal procedures were reviewed and approved by the Osaka University Faculty of Dentistry Intramural Animal Care and Use Committee.

The preparations were essentially as described in detail by Yoshida et al. (1994). In brief, the masseter and mylohyoid nerves were exposed, and bipolar electrodes were placed around them. Bipolar electrodes were also placed in the mandibular canal for stimulation of the inferior alveolar nerve and in the infraorbital canal for stimulation of the infraorbital nerve. Then, animals were placed in a stereotaxic frame, and after a craniotomy, parts of the occipital cortex, tentorium, and cerebellum were removed to expose the brainstem caudal to the inferior colliculi. Cisternal drainage and pneumothorax were performed to reduce pulsations of the brainstem. Animals were then immobilized with pancuronium bromide (0.07 mg/kg, i.v.) and artificially ventilated.

Electrodes and tracers. Intracellular recordings were made using glass microelectrodes (borosilicate glass; 1.5 mm outer diameter), filled with either 5% HRP (Toyobo, Osaka, Japan) or 3% biotinamide [Neurobiotin (Nb); Vector Laboratories, Burlingame, CA], both of which were dissolved in 0.3 M KCl and 0.05 M Tris buffer, pH 7.6. Electrodes filled with HRP were used to make recordings from motoneurons, whereas Nb-filled electrodes were used to record from neurons in the Vo.r. In either case, the electrodes were beveled to resistances of 15–30 MΩ.

Recording and labeling procedures. We first located the Vmo on the basis of the antidromic field potentials that were recorded in response to electrical stimulation of the muscle nerves (single pulse with 0.2 msec duration at 1 Hz) and then identified masseter (JC) and JO motoneurons on the basis of the antidromic spike potentials recorded intracellularly. Injection of HRP into motoneurons (resting potential more negative than −50 mV) was made by using positive DC currents of 15–20 nA applied for 1.5–2.5 min. We only attempted to fill a single masseter and a single JO motoneuron in each animal.

Subsequently, the HRP electrode was withdrawn, and an electrode filled with Nb was inserted into the Vo.r. The Vo.r was located on the basis of both the stereotaxic coordinates and the monosynaptic field potential (mean latency, 1.2 msec) that was elicited by single electrical stimuli applied to either the inferior alveolar nerve or the infraorbital nerve. Intracellular recordings were obtained from Vo.r neurons, with intracellular penetrations being initially identified by the appearance of EPSPs with spike potentials after electrical stimulation of either the inferior alveolar nerve or the infraorbital nerve (single pulse of 0.2 msec duration at 1 Hz). Neurons were characterized physiologically by noting the location of the receptive field and determining the response of the neuron to mechanical stimulation (e.g., tactile stroking of facial skin and oral mucosa, pressing and tapping teeth, and stretching lower jaw). After determining the electrophysiological characteristics of the neuron, Nb was iontophoresed with 10–15 nA positive DC current for 1–2 min, even if the resting membrane potential decreased (less than −40 mV). We only attempted to fill a single Vo.r neuron per animal.

Histochemical procedures. Animals were allowed to survive for 6–12 hr from the time of the last injection, after which they were deeply anesthetized further and perfused through the ascending aorta with 1.5 l of 0.02 M PBS, pH 7.4. Subsequently, animals were perfused with 4 l of fixative solution of 4% paraformaldehyde in 0.1 M phosphate buffer (PB), pH 7.4, followed by 1 l of the same fixative containing 10% sucrose. The brainstem was removed then and placed in 25% sucrose in 0.1 M PB, pH 7.4, at 4°C for 1 week. Transverse serial sections (60 μm thickness) were cut on a freezing microtome. Sections were washed in 0.1 M PBS and processed with 0.04% 3,3′-diaminobenzidine tetrahydrochloride (DAB) and 0.003% H_2O_2 in 0.1 M PB, pH 7.4. Then, they were washed in 0.05 M Tris-buffered saline (TBS), pH 7.6, and incubated overnight at 4°C in streptavidin conjugated with HRP (1:400; Dako, Glostrup, Denmark) in 0.05 M TBS containing 1% Triton X-100. After several rinses with TBS, sections were reacted with 0.02% DAB, 0.003% H_2O_2, and 0.7% nickel ammonium sulfate in 0.05 M Tris buffer, pH 7.6, for 15 min. They were washed then in 0.05 M Tris buffer, pH 7.6, and mounted on slides coated with chrome-alum and gelatin. Finally, they were dried overnight, counter-stained with neutral red, dehydrated in graded alcohols, cleared in xylene, and coverslipped.

Reconstruction of labeled neurons. Motoneurons and axon collaterals of Vo.r neurons that made synaptic contacts were reconstructed from multiple sections using camera lucida. Objectives of 20× or 50× were used (200× or 500× total magnifications; Olympus Optical, Tokyo, Japan). A 100× oil immersion objective was used to reconstruct collateral terminations (1340× total magnification) and to identify points of possible synaptic contact (1000× total magnification). Photomicrographs of the contacts were taken by using a 100× oil immersion objective. As was shown in our previous studies (Yabuta et al., 1996; Yoshida et al., 1999), possible contacts were only accepted if all of the following criteria were satisfied: all stained contacts should be traced back to the stem axon of the labeled Vo.r neuron, the contact should consist of a clear terminal bouton or an en passant bouton, and there should be no gap between the presynaptic and postsynaptic profiles at the same focus (Brown and Fyffe, 1981; Markram et al., 1997). In the present study, Vo.r neurons were injected with Nb, and trigeminal motoneurons were injected with HRP. Premotoneurons and motoneurons were then visualized with and without nickel enhancement, respectively. This technique tinged collaterals and boutons of the Vo.r neurons and the motoneurons with black and light brown, respectively, making it easy to confirm the presence of contacts between the two elements.

Measurements of boutons and somata of motoneurons. Counts of labeled boutons and counter-stained motoneurons in the Vmo were made using a 50× oil-immersion objective (500× total magnification). Counts of the counter-stained neurons were performed using the optical dissector method (Coggeshall and Lekan, 1996), with counting being restricted to the structures with both a clear nucleolus and clearly delineated soma. Small counter-stained neurons with the diameter being <20 μm, which had piriformis-like or spindle-like soma with less number of primary dendrites, were not counted, because those neurons displayed a feature common to intranuclear neurons (Shigenaga et al., 1988b). The soma diameter was measured on a drawing reconstructed in a transverse plane using the 50× oil-immersion lens (500× total magnification). Measurements of bouton diameters were made from camera lucida drawings using the 100× oil-immersion lens (1340× total magnification). These drawings were scanned (at 400 dots per inch) and analyzed using NIH Image (Wayne Rashand, National Institutes of Health, Bethesda, MD). No corrections for tissue shrinkage resulting from fixation and histological procedures were made in this study. Comparisons of the means of two groups were made by the Mann–Whitney U test or Student's t test at the $p = 0.05$ level. Photomicrographs were processed and labeled using Photoshop 5.0J (Adobe Systems, San Jose, CA), with only the contrast being adjusted during processing. Montages were printed on a Fuji Pictography 3000 digital photographic printer (Fuji Photo Film, Tokyo, Japan).

Data from one Vo.r neuron (CL2) with terminals in the Vmo.dl and one Vo.r neuron (OP2) with terminals in the Vmo.vm, which were used for a previous electron microscopic (EM) study (Shigenaga et al., 2000), were included in the present LM analysis. These two neurons had been labeled by HRP injections, and three sections containing the Vmo had been subjected to the EM analysis from each neuron. In these sections, the measurements of numbers of motoneurons, labeled boutons, and contacts on motoneuronal somata were made from polymerized plastic sections before ultrathin sectioning. The remaining sections were analyzed according to the protocols described above.

RESULTS

In the present study, injections of tracers (Nb or HRP, see Materials and Methods) were made into a Vo.r neuron, a masseter motoneuron (JC), and a jaw-opening (JO) motoneuron in

Table 1. Quantitative data for single Vo.r neuron terminals and their contacts on counter-stained motoneuronal somata in the JC motor nucleus and the JO motor nucleus

Case number	Receptive field	Total number of boutons	Number (percentage) of boutons contacted	Total number of motoneuronal somata	Number (percentage) of somata contacted	Number of contacts per soma contacted
Vo.r-dl neurons[a]						
CL1	Lower canine and premolars	6123	1202 (19.6)	1572	278 (17.7)	4.3
CL2	Upper premolars	5855	1168 (19.9)	1656	297 (17.9)	3.9
CL3	Upper premolars	2022	362 (17.9)	1541	112 (7.3)	3.2
CL4	Upper teeth	4565	748 (16.4)	1728	220 (12.7)	3.4
CL5	Lower incisors	3620	450 (12.4)	1674	173 (10.3)	2.6
Mean ± SEM		4437 ± 754*	786 ± 175* (17.2 ± 1.4%)	1634 ± 34*	216 ± 34* (13.2 ± 2.1%)*	3.5 ± 0.3
Vo.r-vm neurons[b]						
OP1	Lower premolars and molars	556	94 (16.9)	521	34 (6.5)	2.8
OP2	Lower incisors	471	75 (15.9)	485	33 (6.8)	2.3
OP3	Upper and lower lips	341	48 (14.1)	474	21 (4.4)	2.3
OP4	Upper and lower premolars and molars	449	71 (15.8)	498	25 (5.0)	2.8
OP5	Upper gingiva between canine and first premolar	406	72 (17.7)	480	24 (5.0)	3.0
Mean ± SEM		445 ± 36*	72 ± 7* (16.1 ± 0.6%)	492 ± 8*	26 ± 3* (5.3 ± 0.6%)*	2.8 ± 0.1

[a]Indicates Vo.r neurons that issue collaterals terminating in JC motor nucleus.

[b] Indicates Vo.r neurons that issue collaterals terminating in JO motor nucleus.

*Significant differences ($p < 0.05$, Mann–Whitney U test) between Vo.r-dl and Vo.r-vm neurons.

each of 39 animals. Twenty-two Nb-labeled Vo.r neurons were found after histochemical processing. Thirteen of these neurons had axon collaterals that terminated in the Vmo.dl of the Vmo (Vo.r-dl neurons) and nine in the Vmo.vm of the Vmo (Vo.r-vm neurons). In the remaining 17 neurons, the labeling was too weak to identify their terminals with a light microscope. Of the 13 Vo.r-dl neurons, 10 each contained an Nb-labeled Vo.r-dl neuron, an HRP-labeled masseter motoneuron, and an HRP-labeled JO motoneuron. In four of the 10 cases, contacts made between the Vo.r-dl neurons (CL1, CL3, CL4, and CL5) and the masseter motoneurons were found, and these four pairs were reconstructed and analyzed. An additional HPR-labeled Vo.r-dl neuron CL2 that was used for a previous EM study (Shigenaga et al., 2000) was added to the present analysis. Of the nine Vo.r-vm neurons, eight contained an Nb-labeled Vo.r-vm neuron, an HRP-labeled JO motoneuron, and an HRP-labeled masseter motoneuron. In two of the eight pairs, contacts were found between the Vo.r-vm neurons (OP1 and OP3) and JO motoneurons, and these two pairs were reconstructed and analyzed. An additional two Vo.r-vm neurons (OP4 and OP5) and an HRP-labeled Vo.r-vm neuron OP2 used for a previous EM study (Shigenaga et al., 2000) were also incorporated in the present analysis.

General physiology and morphology of Vo.r neurons

All Vo.r-dl neurons (CL1, CL2, CL3, CL4, and CL5) were activated when light mechanical stimulation was applied to the teeth. Four neurons (CL1, CL2, CL3, and CL5) were of the fast adapting (FA) type, whereas the other neuron (CL4) was a slowly adapting (SA) type. In contrast, all Vo.r-vm neurons (OP1, OP2, OP3, OP4, and OP5) were the FA type. Neurons OP1, OP2, and OP4 were activated by light mechanical stimulation of the teeth (periodontal ligament), whereas neurons OP3 and OP5 had their receptive field in the lips and gingiva, respectively. The location of their receptive fields is listed in Table 1. Fast-adapting neurons were characterized by their transient response to a tap of the tooth without directional sensitivity, whereas the SA periodontal neuron CL4 responded phasically with directional sensitivity to gentle deformation in one of the four orthogonal directions. The gingival neuron (OP5) and lip neuron (OP3) both displayed a transient response to a maintained light pressure applied to the receptive field. Note that none of the Vo.r neurons examined responded to displacement of the lower jaw, suggesting that these neurons received no input from jaw-muscle spindle afferents.

An example of the electrophysiological and morphological data on a Vo.r-dl neuron CL3 is shown in Figure 1*A–C*. This neuron fired two spikes, superimposed on EPSP, in response to a single electrical stimulation (submaximal) of the infraorbital nerve; the maximal stimulation increased the duration of the EPSP and numbers of the action potentials (data not presented). These firing patterns were applicable to the other Vo.r neurons examined and to previously reported Vo.r neurons (Yoshida et al., 1994; Shigenaga et al., 2000), but the number of action potentials differed from one cell to another (2–9 spikes). This neuron was activated in an FA fashion by a gentle tap applied to upper premolars. The latencies of EPSPs generated in five Vo.r-dl neurons and five Vo.r-vm neurons ranged from 1.2 to 1.7 msec (mean, 1.4 msec) after a single electrical stimulation of the peripheral nerve. As was previously reported (Yoshida et al., 1994; Shigenaga et al., 2000), Vo.r neurons were arranged in a topographic fashion with the somata of Vo.r-dl neurons being located more dorsally or laterally than those of Vo.r-vm neurons (Fig. 1*D*,*E*). In addition, we confirmed our earlier observation (Yoshida et al., 1994) that Vo.r neurons issue collaterals that terminate in the brainstem nuclei other than the Vmo [e.g., principal nucleus (Vp), Vo, intertrigeminal region, and juxtatrigeminal region]. Detailed observation of axonal trajectory in regions other than the Vmo and complete reconstructions of examined Vo.r neurons except for a Vo.r-dl neuron CL3 (Fig. 1*B*,*C*), however, were not performed.

Contacts made by single Vo.r neurons and single motoneurons

Contacts on JC motoneurons

The masseter motoneurons were identified by intracellular recordings of antidromic responses after stimulation of the masseter nerve. Antidromic spike potentials of the four masseter motoneu-

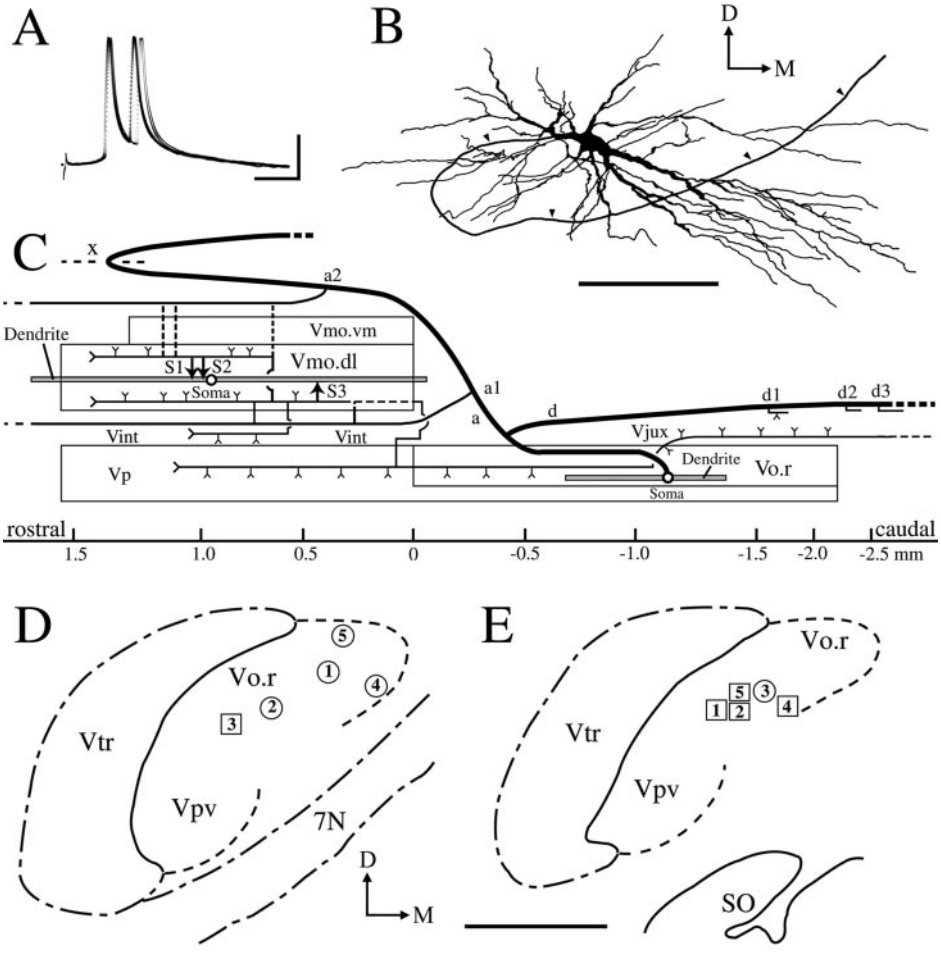

Figure 1. Physiology and morphology of a labeled neuron CL3 in the rostrodorsomedial part (*Vo.r*) of oral nucleus (*A–C*) and the somal location of labeled Vo.r neurons examined (*D*, *E*). *A*, Eight superimposed *traces* of intracellular potentials recorded from the Vo.r neuron CL3 after stimulation of the infraorbital nerve with submaximal intensity. *B*, Camera lucida drawings of soma-dendrites and part of the stem axon (*arrowheads*) of the Vo.r neuron. *C*, Diagram of axonal trajectory of the Vo.r neuron with terminals in the dorsolateral division (*Vmo.dl*) of the trigeminal motor nucleus (Vmo) and in the brainstem nuclei other than the Vmo.dl. Contacts made between the Vo.r neuron and labeled masseter motoneuron are marked with *arrowheads* labeled by *S1*, *S2*, and *S3*. The collaterals from an ascending and a descending axon are denoted by *a* and *d*, respectively. *X* indicates the midline. *D*, *E*, Somal location of Vo.r neurons examined is plotted in two sections at the rostral (*D*) and caudal (*E*) levels of the Vo.r. *Circles* and *squares* represent Vo.r neurons that project to the Vmo.dl and to the ventromedial division (*Vmo.vm*) of the Vmo, respectively. *Arabic numerals* within the *circles* and *squares* indicate sample (neuron) numbers. *SO*, Superior olive; *Vint*, intertrigeminal region; *Vjux*, juxtatrigeminal region; *Vp*, trigeminal principal nucleus; *Vpv*, ventrolateral subnucleus of Vp; *Vtr*, spinal trigeminal tract; *7N*, facial nerve; *D–M*, dorsal–medial. Calibration: *A*, 10 mV, 4 msec. Scale bars: *B*, 2 mm; *D*, *E*, 1 mm.

rons were evoked at a constant latency of 0.6–0.8 msec (mean, 0.7 msec), which compares to a mean latency of 0.8 msec reported for a sample of 23 intracellularly labeled α-masseter motoneurons (Yabuta et al., 1996). In one of the four masseter motoneurons (initial membrane potential, −62 mV), we observed a depolarizing hump in the membrane potential (Chandler et al., 1994; Kobayashi et al., 1997) that separated the first from slow afterhyperpolarization (also see Shigenaga et al., 1988b, 2000). The soma diameters of the four masseter motoneurons ranged from 41.4 to 53.9 μm with a mean of 47.7 μm, and thus belong to a large-sized group of masseter motoneuron (see Fig. 9*A*). Four of the 10 pairs of Vo.r-dl neuron–JC motoneuron combinations established contacts (see Materials and Methods for the criteria of the contacts). The number of contacts made by each pair was 4 (CL1), 3 (CL3), 7 (CL4), and 6 (CL5), respectively, with a mean of 5 ($\pm$ 0.9, SEM). One pair (CL4) made contacts on the soma and proximal dendrites, but the other pairs contacted only dendrites. Dendritic contacts were located within 550 μm from the soma, with the exception of contacts made by one pair (CL5), which occurred more distally (Fig. 2). Note that each of the labeled boutons never contacted two different postsynaptic profiles.

Figure 3 shows the superimposed drawings that were reconstructed from a Vo.r-dl neuron CL3 and a masseter motoneuron. This premotoneuron issued a stem axon that divided into an ascending and a descending axon (Fig. 1*C*). The ascending axon issued two collaterals, a1 and a2, that formed terminal arbors in the Vmo.dl. The collateral a1 bore a terminal bouton (*S3*) that made a contact on a caudoventrally directed fourth-order dendrite of the masseter motoneuron. The collateral a2 bore two en passant boutons that contacted on a ventrally extended fourth-order dendrite (*S1*) and on a dorsomedially extended second-order dendrite (*S2*), respectively. The physical distance and location of the individual contacts are diagrammatically illustrated in Figure 2*B*.

An example of contacts made by a Vo.r-dl neuron CL4 on the soma and proximal dendrites of a masseter (JC) motoneuron is illustrated in Figure 4. In this figure, parts of the motoneuron and collateral branches that constituted contacts were reconstructed. This Vo.r-dl neuron CL4 had an ascending stem axon only, which gave off two collaterals a1 and a2 terminating in the Vmo.dl, but the contacts were made by boutons given off from the collateral a2 only. Specifically, two en passant boutons (S4, S5) contacted a rostromedially directed first-order dendrite (Figs. 2*C*, 4*A*), one en passant bouton (S6) contacted a rostrodorsolaterally directed first-order dendrite (not illustrated in Fig. 4), and one terminal bouton (S7) contacted a dorsally directed second-order dendrite of the motoneuron (Figs. 2*C*, 4*B*). The collateral a2 also gave off two terminal boutons (S1, S2) and one en passant bouton (S3), all of which formed contacts on the soma of the motoneuron (Figs. 2*C*, 4*A*).

Contacts on JO motoneurons

The JO motoneurons were identified by intracellular recordings of antidromic responses after stimulation of the mylohyoid nerve. Antidromic spike potentials of the two JO motoneurons were

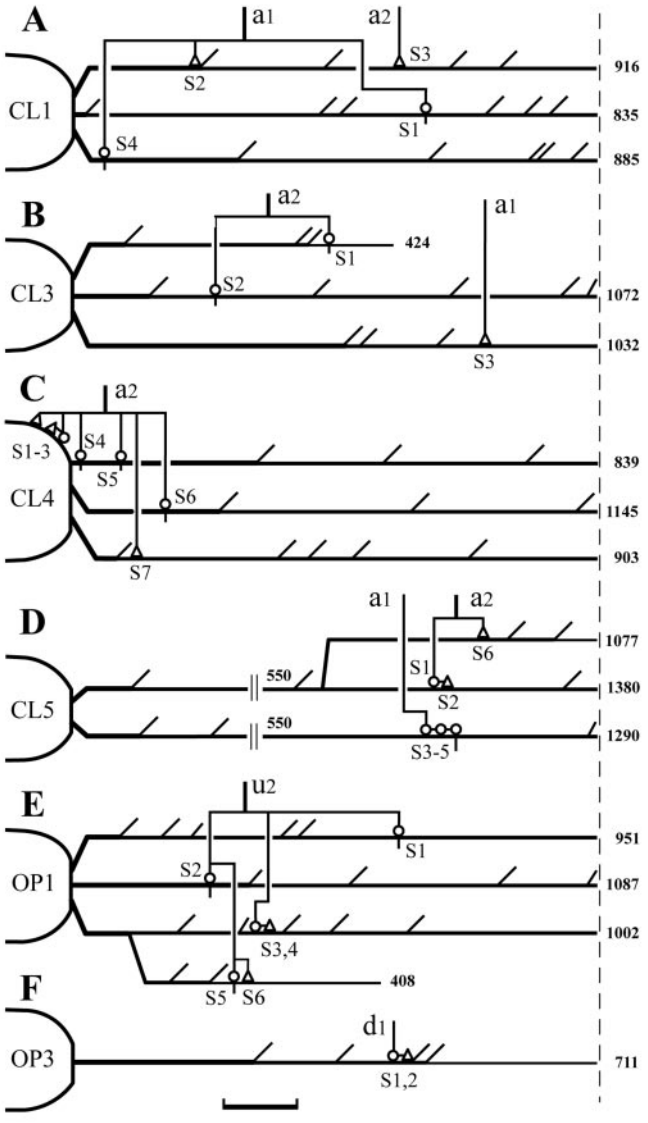

Figure 2. Diagrammatic summary showing the locations of contacts made by four Vo.r-dl neuron–JC motoneuron pairs (*A–D*) and two Vo.r-vm neuron–JO motoneuron pairs (*E*, *F*), with terminal boutons denoted by *open triangles* and en passant boutons denoted by *open circles*. JC and JO motoneurons receiving contacts from single Vo.r neurons are marked with *CL* and *OP*, respectively. In each pair, contacts marked with *Sn* are arbitrary. Scale bar, 100 μm (refers to the geometric dendritic distance from the soma). The distance was measured from reconstructions in the transverse plane and corrected by using the Pythagorean theorem and the section thickness. The *a*, *d*, and *u* indicate collaterals given off from an ascending fiber, a descending fiber, and a stem axon, respectively. Dendrites longer than 700 μm in *A–C*, *E*, and *F* and those longer than 1000 μm in *D* are interrupted with a *broken line. Arabic numerals* attached to the end of *dendritic lines* indicate the longest distance (μm) of the dendritic tree formed by each primary dendrite. Note that the second *dendritic line* in *D* starts 550 μm from the soma. The axon collateral branching patterns and somata are also shown, but not to scale. For further descriptions, see Results.

evoked at a constant latency of 0.92 and 0.63 msec, respectively (note that a depolarizing hump was not seen). Their somal diameters were 52.1 and 45.7 μm, respectively. Two of the six pairs of Vo.r-vm neuron–JO motoneuron combinations established two and six contacts, respectively. All contacts made by the two pairs were located within the proximal two-thirds of dendrites (Fig. 2*E*,*F*). Each of the labeled boutons made a single contact on a dendrite.

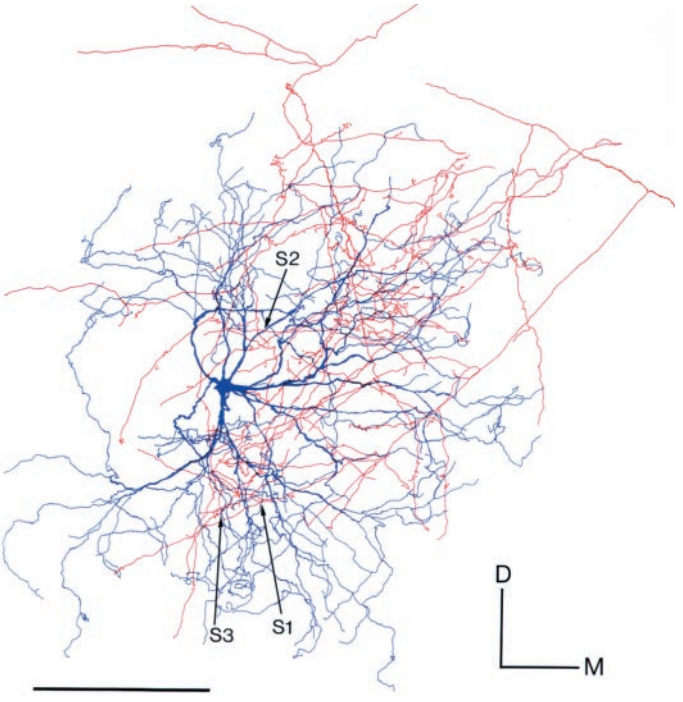

Figure 3. Camera lucida drawings reconstructed from a labeled masseter motoneuron (*blue*) and a labeled Vo.r neuron CL3 (*red*) showing three contacts made between the two. Contacts are marked with *arrows* labeled with *S1*, *S2*, and *S3*. The size of labeled boutons drawn is exaggerated. Note that the intracellular responses, soma-dendrites and a stem axon, and scheme of the axonal trajectory of the Vo.r neuron are shown in Figure 1*A–C*, respectively. *D–M*, Dorsal–medial. Scale bar, 0.4 mm.

An example of contacts made by a Vo.r-vm neuron OP1 on a JO motoneuron is illustrated in Figures 5 and 6. This pair involved a total of six contacts. Figure 5 shows the superimposed drawings that were reconstructed from the Vo.r-vm neuron OP1 and the JO motoneuron. In Figure 6, parts of the collateral branches and dendrites that formed contacts were reconstructed, but note that two contacts, S1 and S2, are not shown. This Vo.r-vm neuron OP1 had a stem axon that divided into an ascending and a descending axon. One collateral u2 (united axon) given off from the stem axon arising from the soma formed terminal arbors in the Vmo.vm and branched extensively, especially in the ventral part of Vmo.vm. This collateral made six contacts on dendrites of the motoneuron, with four of the contacts being from en passant boutons and two from terminal boutons (Figs. 2*E*, 5, 6). An en passant bouton (S1) contacted a rostroventrally directed sixth-order dendrite, whereas another (S2) contacted a rostrally directed first-order dendrite. In addition, an en passant bouton (S3) and a terminal bouton (S4) both made contact on the same, rostromedially directed, fourth-order dendrite (Figs. 2*E*, 5, 6*A*). The remaining en passant bouton (S5), together with a terminal bouton (S6), contacted another rostroventrally directed fourth-order dendrite (Figs. 2*E*, 5, 6*B*) that arose from the same primary dendrite as that for the contacts S3 and S4.

Contacts made by single Vo.r neurons on counterstained motoneuronal somata

General morphology

Axon collateral(s) of the Vo.r neurons gave off boutons that appeared to form numerous patch-like clusters distributed widely

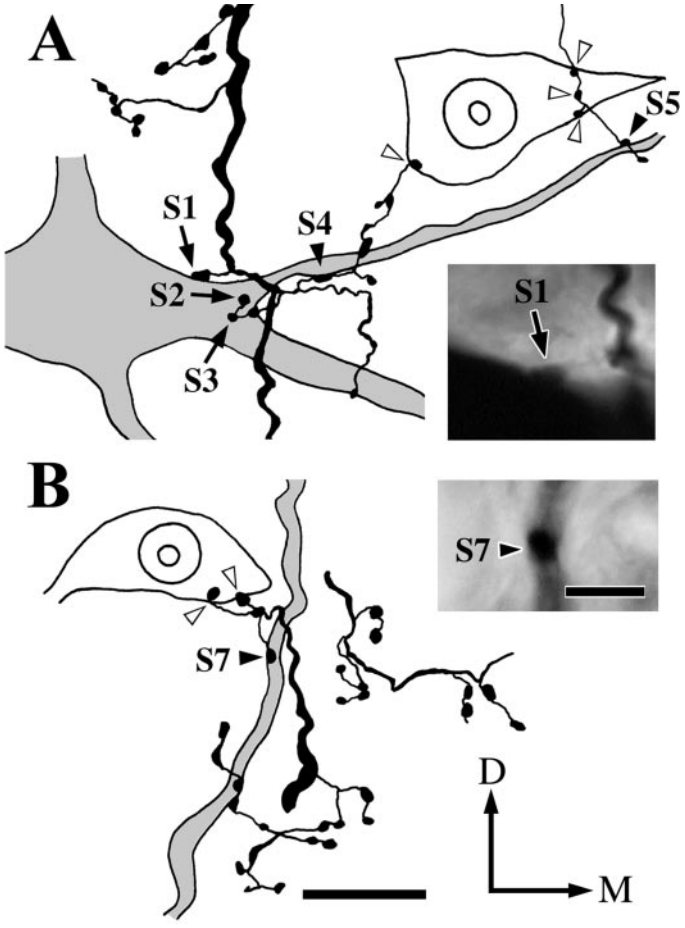

Figure 4. Parts of drawings reconstructed from a labeled Vo.r neuron CL4 and a labeled masseter motoneuron showing six contacts (*S1–5* and *S7*) and photomicrographs of the contacts *S1* and *S7*. *A*, Contacts made by labeled boutons from the Vo.r neuron on the soma (*S1*, *S2*, and *S3*, *arrows*) and a primary dendrite (*S4* and *S5*, *filled arrowheads*) of the labeled masseter motoneuron and on a counter-stained motoneuronal soma (*open arrowheads*) in the Vmo.dl. Photomicrograph in the *inset* shows the contact *S1* (*arrow*). *B*, Contacts made by a labeled bouton on a proximal dendrite (*S7*, *filled arrowhead*) of the labeled motoneuron and two labeled boutons on the soma of a counter-stained motoneuron (*open arrowheads*) in the Vmo.dl. Photomicrograph in the *inset* shows the contact *S7* (*filled arrowhead*). A contact S6 is not included in sections used for the reconstructions. Note that the labeled soma and the counter-stained somata are cut into two pieces, and each contact is seen on the surface of a smaller piece. *D–M*, Dorsal–medial. Scale bars: reconstructions *A* and *B*, 20 μm; insets *A* and *B*, 5 μm.

in either the Vmo.dl (Fig. 7*A–C*) or Vmo.vm (Fig. 7*D*–F). Of these boutons, significant numbers were found to contact the somata (Fig. 8*A*) and/or juxtasomatic regions (Fig. 8*B*) of motoneurons stained with neutral red.

The boutons of both Vo.r-dl and Vo.r-vm neurons consisted of an en passant type and a terminal type. A total of 1022 boutons sampled randomly from the three Vo.r-dl (CL1, CL4, and CL5) and two Vo.r-vm neurons (OP1, OP3) showed a similar proportion of en passant boutons and terminal boutons: ~60% (618/1022) were of en passant type, and measurements of the diameters of 256 boutons showed no difference for boutons of the en passant and terminal type. However, the diameter of a sample of 908 boutons randomly selected from the three Vo.r-dl neurons was 1.7 ± 0.0 μm (mean ± SEM), which was significantly smaller

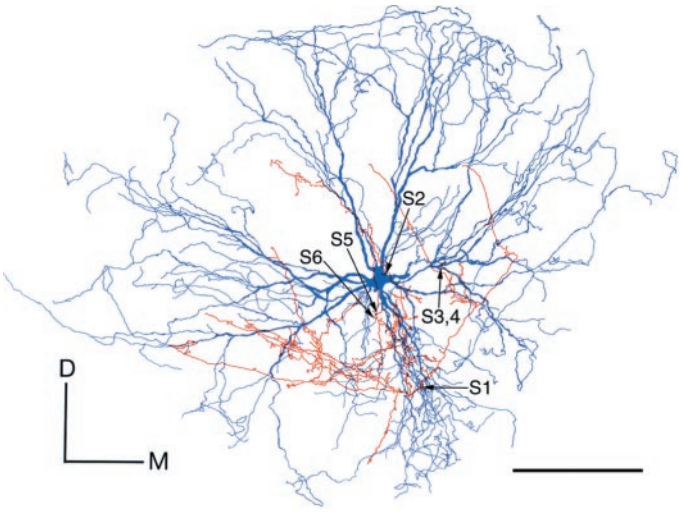

Figure 5. Camera lucida drawings reconstructed from a labeled jaw-opening (JO) motoneuron and a labeled Vo.r neuron OP1 showing six contacts made between the two. Contacts are marked with *arrows* labeled with *S1*, *S2*, *S3*, *S4*, *S5*, and *S6*. The size of labeled boutons drawn is exaggerated. *D–M*, Dorsal–medial. Scale bar, 0.4 mm.

than that of a sample of 228 boutons randomly selected from the two Vo.r-vm neurons (1.9 ± 0.0 μm).

Quantitative analysis

Contacts made by the five Vo.r-dl neurons (CL1, CL2, CL3, CL4, and CL5) and five Vo.r-vm neurons (OP1, OP2, OP3, OP4, and OP5) on counter-stained somata were analyzed (Table 1). The average number of boutons given off from single Vo.r-dl neurons was 9.7 times higher than that from single Vo.r-vm neurons. The average number of somatic contacts made by the Vo.r-dl neurons was 11 times higher than that made by the Vo.r-vm neurons, which rendered a significantly higher proportion of the number of somata contacted for the Vo.r-dl neurons than for the Vo.r-vm neurons. The number of contacts per motoneuronal soma was, on average, 3.5 and 2.8 for the Vo.r-dl and Vo.r-vm neurons, respectively, but this difference was not significant.

Because the JC motor nucleus contains α- and γ-motoneurons, in contrast to the JO one that contains α-motoneurons only, the soma diameters of counter-stained JC and JO motoneurons in cases CL5 and OP3, respectively, were measured. The soma diameters of JC motoneurons showed an asymmetric distribution that was skewed to the peak value (Fig. 9*A*), whereas those of JO motoneurons were unimodally distributed (Fig. 9*B*). Although the somata in the JC motor nucleus were significantly larger than those in the JO motor nucleus [42.0 ± 0.3 μm (n = 625) vs 36.0 ± 0.3 μm (n = 370)], the different distribution patterns indicate that γ-motoneurons are contained within the smallest group of the JC motoneuron. This suggests that soma sizes of JO α-motoneurons and JC γ-motoneurons partly overlap each other. Judging from the size distribution of somata contacted (closed columns in Fig. 9*A*) in the JC motor nucleus, JC motoneurons involved in the small group receive less frequent contacts from terminals of Vo.r-dl neurons. Note that each of the labeled boutons never contacted two different counter-stained somata.

DISCUSSION

Intracellular labeling of single second-order sensory neurons in the Vo.r and single trigeminal motoneurons revealed that two

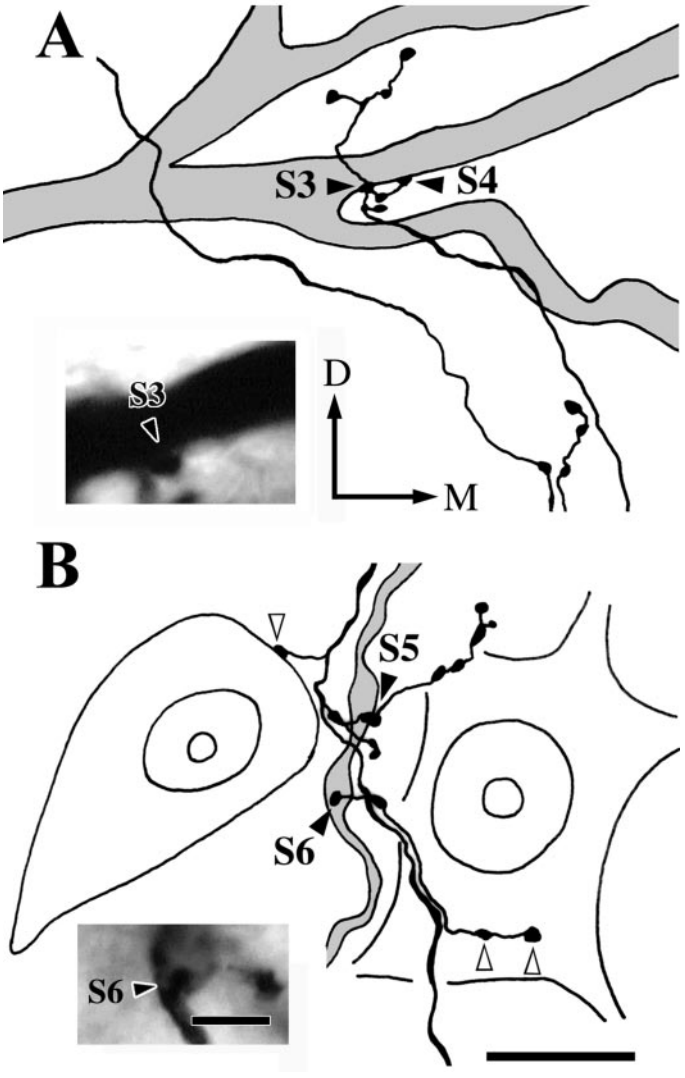

Figure 6. Parts of drawings illustrated in Figure 5 showing the contacts *S3* and *S4* (*A*) and the contacts *S5* and *S6* (*B*) at higher magnification and photomicrographs of the contacts *S3* and *S6*. *A*, Contacts made by two labeled boutons on the same dendrite of the labeled JO motoneuron (*S3* and *S4*, *filled arrowheads*). Photomicrograph in the *inset* shows the contact *S3* (*filled arrowhead*). *B*, Contacts made by two labeled boutons on the same dendrite of the labeled motoneuron (*S5* and *S6*, *filled arrowheads*). Photomicrograph in the *inset* shows the *S6* contact (*filled arrowhead*). Note that labeled boutons make contacts with the soma of two counter-stained JO motoneurons (*open arrowheads*). *D–M*, Dorsal–medial. Scale bars: reconstructions *A* and *B*, 20 μm; insets *A* and *B*, 5 μm.

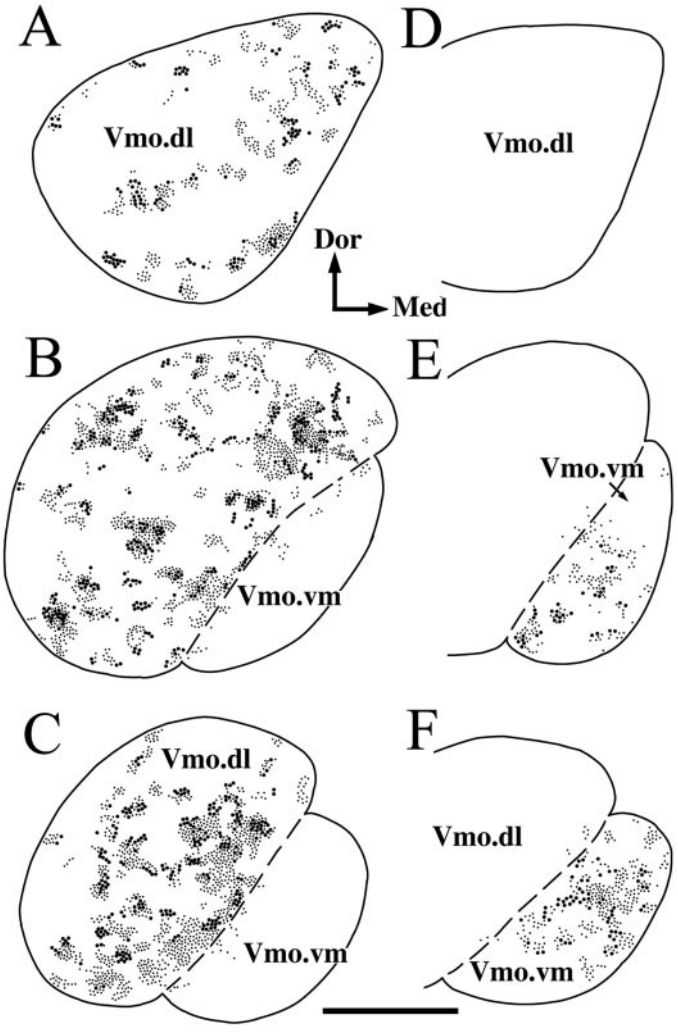

Figure 7. Distribution patterns of labeled boutons from a Vo.r neuron CL1 in the Vmo.dl (Vo.r-dl neuron; *A–C)* and from a Vo.r neuron OP1 in the Vmo.vm (Vo.r-vm neuron; *D–F*). The Vo.r-dl neuron boutons found in every alternate section at levels of the rostral (*A*), middle (*B*), and caudal one-third (*C*) of the Vmo are superimposed in one representative section, respectively. The Vo.r-vm neuron boutons found in serial sections at the rostral (*D*), middle (*E*), and caudal (*F*) levels of the Vmo are superimposed in one representative section, respectively. Boutons contacting the somata and/or juxtasomatic regions of counter-stained motoneurons are marked with *large dots*. Boutons without contacts on the counter-stained motoneurons are marked with *small dots. Dor–Med*, Dorsal–medial. Scale bar, 0.5 mm.

kinds of neuron are connected monosynaptically with a range of 2–7 synaptic sites. The premotoneuron gave off two types of axonal branches: one innervating the soma–dendritic compartment and the other dendrites of the motoneurons. Premotoneurons innervating JC motoneurons show a stronger degree of divergence than those innervating JO motoneurons. The functional implications of neural circuits made between trigeminal sensory and motor neurons are discussed.

Technical considerations

In the present LM observation, one possible limitation is the lack of confirmation that a closed apposition represents a synapse at the EM level. In this respect, we confirmed that axon varicoses forming these close appositions are synapses in a previous EM study (Shigenaga et al., 2000).

Another problem is that the soma size of counter-stained JC motoneurons did not show a clear bimodal distribution. It is, however, possible to consider that γ-motoneurons are contained in the smallest group of the JC motoneurons. Because the morphologic and physiologic criteria for distinguishing β- from α-motoneurons have not been determined in the trigeminal JC motoneurons, we did not take β-motoneurons into consideration in the present study.

Comparisons of contacts made by premotoneurons on JC and JO motoneurons

In the present study, two approaches were used to provide direct evidence on the location and number of Vo.r neuron terminations on trigeminal motoneurons. We combined HRP injections into

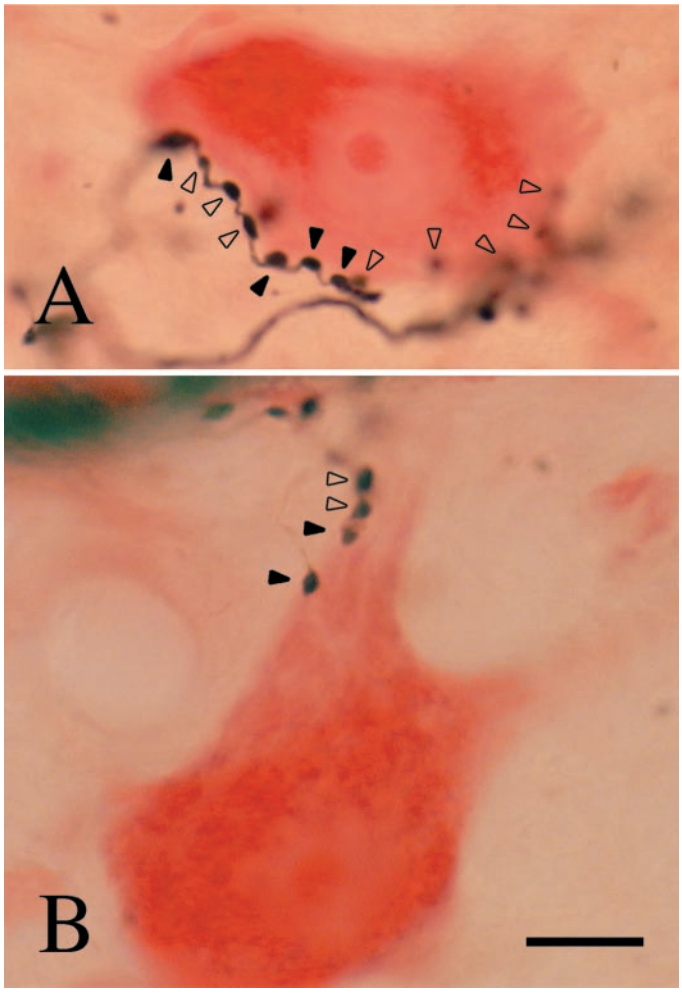

Figure 8. Photomicrographs showing contacts made by a labeled Vo.r-dl neuron CL1 on the soma (*A*) and the juxtasomatic region (*B*) of counter-stained motoneurons. *Filled arrowheads* denote contacts that are relatively in focus. Contacts marked with *open arrowheads* are out of focus but could be identified by adjusting the focus. Scale bar, 20 μm.

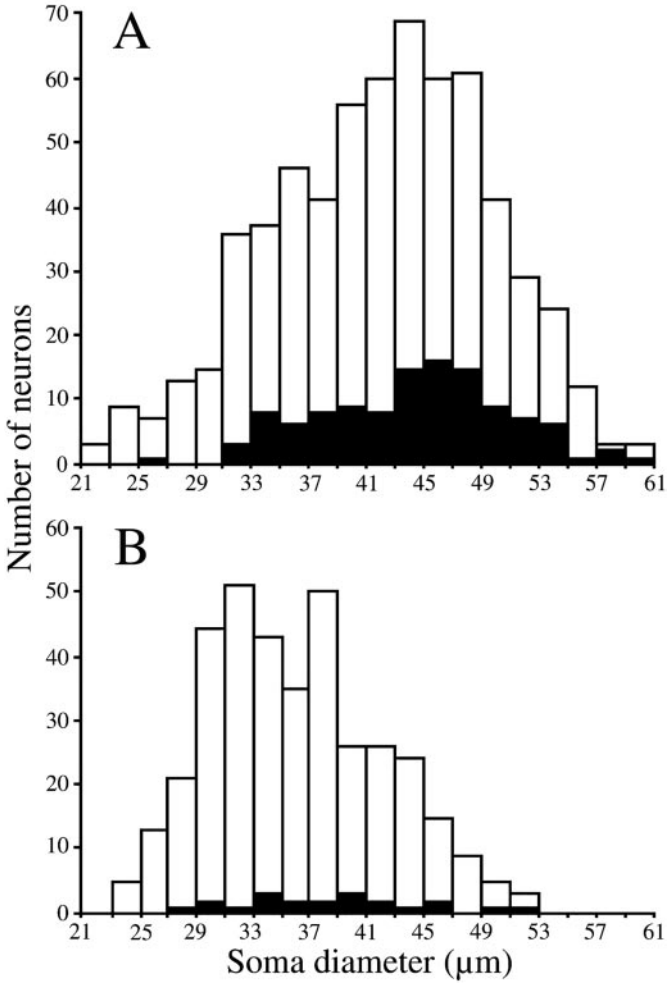

Figure 9. Size distributions of counter-stained somata without contacts (*open columns*) and with contacts (*filled columns*) in the JC (*A*) and the JO (*B*) motor nucleus. The somata measured were randomly selected from sections in case Vo.r-dl neuron CL5 and in case Vo.r-vm neuron OP3.

single JC and JO α-motoneurons with Nb injections into single Vo.r neurons. This particular combination allowed determination of the number and location of contacts on the complete dendritic tree of either JC or JO α-motoneurons. We observed that Vo.r-dl neurons gave off 10 times more boutons than Vo.r-vm neurons, indicating that the proportion of motoneurons receiving contacts is higher for JC than JO motoneurons. Interestingly, the average number of contacts made by Vo.r neurons on α-motoneurons was almost the same between the two kinds of pairs. However, in a previous EM study (Shigenaga et al., 2000), we found that vesicle number and density are significantly higher in synaptic boutons from Vo.r-dl than Vo.r-vm neurons. These results suggest that the synaptic efficacy exerted by a Vo.r-dl neuron is stronger than that by a Vo.r-vm neuron. Furthermore, on average, 17.2 and 16.1% of boutons from single Vo.r-dl and Vo.r-vm neurons contacted 13.2 and 5.3% of counter-stained JC and JO motoneurons (soma and juxtasomatic regions) with 3.5 and 2.8 contacts per soma, respectively. These results imply that the mean value of the number of somata contacted is higher for JC than JO motoneurons.

In addition, the present study made it possible to predict the number of motoneurons that receive contacts from the individual Vo.r neurons. An average number of contacts made between a Vo.r neuron and a motoneuron could be determined as 5.0 for JC α-motoneurons and as 4.0 for JO motoneurons. These values, combined with a total number of JC or JO motoneurons obtained from each case, render such prediction that, on average, a Vo.r-dl neuron terminates on 887 (± 151; range, 404–1225 neurons) JC motoneurons, which covers 54.2% (± 9.3%; range, 26.2–77.9%) of the total number of JC motoneurons. On the other hand, on average, a Vo.r-vm neuron ends on 111 (± 9; range, 85–139 neurons) JO motoneurons, which covers 22.5% (± 1.5%; range, 17.9–26.7%) of the total number of JO motoneurons. This difference renders the prediction that the proportion of motoneurons contacted is 2.4 times higher for JC than JO motoneurons.

Together, the present results indicate that the net effects of Vo.r neurons exerted on trigeminal motoneurons are much greater for the JC than JO motoneuron pool and suggest that the strength of unitary inputs from single Vo.r neurons to single motoneurons is also stronger for JC motoneurons.

Another important observation of the present study was that every labeled bouton from Vo.r neurons never made contacts with different dendrites of the same motoneuron or with different somata. This finding provides evidence that multiple contacts made by a labeled bouton from Vo.r neurons observed in a

previous EM study (Shigenaga et al., 2000) are made between the bouton and different motoneurons.

Comparisons of contacts made by Vo.r neurons and muscle spindle afferents on JC motoneurons

Because recent studies established that jaw-muscle spindle afferents use glutamate as the transmitter (Chandler, 1989) and their terminals represent features common to excitatory synapses (Bae et al., 1996; Luo and Dessem, 1999), comparisons of data on jaw-muscle spindle afferents with those of premotoneurons presented here are important. In previous studies (Yabuta et al., 1996; Yoshida et al., 1999), we injected HRP into single jaw-muscle spindle afferents and single JC α-motoneurons and found that most contacts (90%) are within 600 μm from the soma. The number of contacts located within 200 μm of the dendritic tree is approximately two times higher for the Vo.r-dl neurons than jaw-muscle spindle afferents (53.6 vs 24.2%). This reflects that peripherally induced IPSPs can be reversed by hyperpolarizing current or chloride ions injected into the soma (Shigenaga et al., 1988b). In addition, the number of contacts made on single JC α-motoneurons is higher for Vo.r neurons than jaw-muscle spindle afferents (5.0 vs 2.1) (Yabuta et al., 1996; Yoshida et al., 1999). In contrast to Vo.r-dl neurons, no somatic contacts were found in 20 pairs of a jaw-muscle spindle afferent and a JC α-motoneuron (Yabuta et al., 1996; Yoshida et al., 1999). However, ~4% of boutons from single jaw-muscle spindle afferents were found to make contacts with counter-stained JC motoneuronal somata [data from a study of Yoshida et al. (1999)]. The other difference is that the total number of boutons is five (masseter) and six (temporalis) times lower in single jaw-muscle spindle afferents (Shigenaga et al., 1990; Yoshida et al., 1999) than in single Vo.r-dl neurons. The comparison described above makes it apparent that the synaptic organization made by inhibitory interneurons and primary afferents is very different.

Functional implications

The present study demonstrates that axonal branches of Vo.r neurons are composed of two types: one innervating the soma–dendritic compartment and the other dendrites only, with relatively few synaptic sites. In the cerebral cortex, Buhl et al. (1994), Miles et al. (1996), and Tamás et al. (1997), by using dual recordings and labeling, demonstrated three types of GABAergic interneurons synapsing on pyramidal cells and suggested that basket cells regulate efferent signaling, whereas dendrite-targeting cells control the efficacy of excitatory afferent inputs selectively. This mechanism may be applicable to synaptic actions that were exerted by Vo.r neurons on trigeminal motoneurons presented here. A support for this suggestion is that peripherally and Vo.r-induced IPSPs in JC motoneurons consist of fast and slow components (Shigenaga et al., 2000). It must be noted that to our knowledge premotoneurons innervating the initial segment of the axon, like axo-axonic cells (Somogyi et al., 1983), have not been found in the spinal cord and brainstem.

Furthermore, the present study suggests that periodontal Vo.r premotoneurons play an important role for protecting the oral and craniofacial structures from damages by suppressing activation of trigeminal motoneurons, mainly of JC motoneurons. This suggestion is not in contrast to previously proposed hypotheses by Taylor (1990) indicating that periodontal low-threshold mechanoreceptors provide force feedback regulation of JC motoneurons. The reason is as follows. First, activation of periodontal afferents, with cell bodies located in the mesencephalic trigeminal nucleus (Vmes), can excite JC motoneurons because their axon collaterals terminate in the JC motor nucleus in addition to the supratrigeminal nucleus, intertrigeminal region, and Vp (Shigenaga et al., 1989), where excitatory premotoneurons are located (Turman and Chandler, 1994; Kolta, 1997; Yoshida et al., 1998). Second, a prior EM study (Bae et al., 1996) revealed that periodontal Vmes afferent terminals make synaptic contacts with distal dendrites of JC motoneurons. Third, Yoshida et al. (1998) demonstrated that periodontal Vp neurons with their axons traveling in the trigemino–thalamic tracts, which are presumed to receive input from Vmes periodontal afferents, issue axon collaterals in the JC motor nucleus. Finally, it has been reported that sensitivity of periodontal mechanoreceptors depends on the amount to which the receptors are stretched during tooth movement, i.e., thresholds fall progressively from the fulcrum to the apex (Cash and Linden, 1982); and that periodontal afferent terminals from the Vmes are concentrated to the base of the roots, whereas those from the trigeminal ganglion (TG) are most numerous around the middle of the roots (Byers and Dong, 1989), thus, indicating that thresholds of periodontal afferents are lower for Vmes than TG afferents. In other words, activation of low-threshold periodontal afferents precedes that of higher-threshold ones when the teeth come together or in contact with hard food. We concluded that low-threshold Vmes periodontal afferents provide a positive force feedback regulation of JC motoneurons, whereas activation of high-threshold (not noxious) TG afferents arrests chewing via inhibitory premotoneurons like Vo.r neurons presented here. However, nonperiodontal Vo.r-vm neurons may have different functions; e.g., lip neurons may play a role in keeping food within the mouth.

REFERENCES

Arvidsson J, Gobel S (1981) An HRP study of the central projections of primary trigeminal neurons which innervate tooth pulps in the cat. Brain Res 210:1–16.

Bae YC, Nakagawa S, Yabuta NH, Yoshida A, Pil PK, Moritani M, Chen K, Takemura M, Shigenaga Y (1996) Electron microscopic observations of synaptic connections of jaw-muscle spindle and periodontal afferent terminals in the trigeminal motor and supratrigeminal nuclei in the cat. J Comp Neurol 374:421–435.

Brown AG, Fyffe REW (1981) Direct observations on the contacts made between Ia afferent fibres and alpha-motoneurones in the cat's lumbosacral spinal cord. J Physiol (Lond) 313:121–140.

Buhl EH, Halasy K, Somogyi P (1994) Diverse sources of hippocampal unitary inhibitory postsynaptic potentials and the number of synaptic release sites. Nature 368:823–828.

Burke RE, Glenn LL (1996) Horseradish peroxidase study of the spatial and electrotonic distribution of group Ia synapses on type-identified ankle extensor motoneurons in the cat. J Comp Neurol 372:465–485.

Burke RE, Walmsley B, Hodgson JA (1979) HRP anatomy of group Ia afferent contacts on alpha motoneurones. Brain Res 160:347–352.

Byers MR, Dong WK (1989) Comparison of trigeminal receptor location and structure in the periodontal ligament of different types of teeth from the rat, cat and monkey. J Comp Neurol 279:117–127.

Cash RM, Linden RW (1982) The distribution of mechanoreceptors in the periodontal ligament of the mandibular canine tooth of the cat. J Physiol (Lond) 330:439–447.

Chandler SH (1989) Evidence for excitatory amino acid transmission between mesencephalic nucleus of V afferent and jaw closer motoneurons in guinea-pig. Brain Res 477:252–264.

Chandler SH, Hsaio CF, Inoue T, Goldberg LJ (1994) Electrophysiological properties of guinea pig trigeminal motoneurons recorded in vitro. J Neurophysiol 71:129–145.

Coggeshall RE, Lekan HA (1996) Methods for determining numbers of cells and synapses: a case for more uniform standards of review. J Comp Neurol 364:6–15.

Fyffe REW (1991) Spatial distribution of recurrent inhibitory synapses on spinal motoneurons in the cat. J Neurophysiol 65:1134–1149.

Kishimoto H, Bae YC, Yoshida A, Moritani M, Takemura M, Nakagawa S, Nagase Y, Wada T, Sessle BJ, Shigenaga Y (1998) Central distribution of synaptic contacts of primary and secondary jaw muscle spindle afferents in the trigeminal motor nucleus of the cat. J Comp Neurol 391:50–63.

Kobayashi M, Inoue T, Matsuo R, Masuda Y, Hidaka O, Kang Y, Morimoto T (1997) Role of calcium conductances on spike afterpotentials in rat trigeminal motoneurons. J Neurophysiol 77:3273–3283.

Kolta A (1997) In vitro investigation of synaptic relations between interneurons surrounding the trigeminal motor nucleus and masseteric motoneurons. J Neurophysiol 78:1720–1725.

Luo P, Dessem D (1995) Inputs from identified jaw-muscle spindle afferents to trigeminathalamic neurons in the rat: a double-labeling study using retrograde HRP and intracellular biotinamide. J Comp Neurol 353:50–66.

Luo P, Dessem D (1999) Ultrastructural anatomy of physiologically identified jaw-muscle spindle afferent terminations onto retrogradely labeled jaw-elevator motoneurons in the rat. J Comp Neurol 406:384–401.

Luo P, Wong R, Dessem D (1995) Projection of jaw-muscle spindle afferents to the caudal brainstem in rats demonstrated using intracellular biotinamide. J Comp Neurol 358:63–78.

Lüscher HR, Clamann HP (1992) Relation between structure and function in information transfer in spinal monosynaptic reflex. Physiol Rev 71:71–99.

Markram H, Lübke J, Frotscher M, Roth A, Sakmann B (1997) Physiology and anatomy of synaptic connections between thick tufted pyramidal neurones in the developing rat neocortex. J Physiol (Lond) 500:409–440.

Miles R, Toth K, Gulyas AI, Hajos N, Freund TF (1996) Differences between somatic and dendritic inhibition in the hippocampus. Neuron 16:815–823.

Moritani M, Yoshida A, Honma S, Nagase Y, Takemura M, Shigenaga Y (1998) Morphological differences between fast and slowly adapting lingual afferent terminations in the principal and oral nuclei in the cat. J Comp Neurol 396:64–83.

Olsson KÅ, Westberg KG (1991) Integration in the trigeminal premotor interneurones in the cat. 2. Functional characteristics of neurones in the subnucleus-γ of the oral nucleus of the spinal trigeminal tract with a projection to the digastric motoneurone subnucleus. Exp Brain Res 84:115–124.

Rall W (1977) Core conductor theory and cable properties of neurons. In: The nervous system, Vol I, Cellular biology of neuron, Pt 1 (Kandel ER, ed) pp 39–97. Bethesda, MD: American Physiological Society.

Rall W, Burke RE, Nelson PG, Smith TG, Frank K (1967) The dendritic location of synapses and possible mechanisms for the monosynaptic EPSP in motoneurons. J Neurophysiol 30:1169–1193.

Redman SJ (1979) Junctional mechanisms at group Ia synapses. Prog Neurobiol 12:33–83.

Redman SJ, Walmsley B (1983) The time course of synaptic potentials evoked in cat spinal motoneurons at identified group Ia synapses. J Physiol (Lond) 343:117–133.

Shigenaga Y, Okamoto T, Nishimori T, Suemune S, Nasution ID, Chen IC, Tsuru K, Yoshida A, Tabuchi K, Hosoi M, Tsuru H (1986a) Oral and facial representation in the trigeminal principal and rostral spinal trigeminal nuclei of the cat. J Comp Neurol 244:1–18.

Shigenaga Y, Suemune S, Nishimura M, Nishimori T, Sato H, H Ishidori, Yoshida A, Tsuru K, Tsuiki Y, Dateoka Y, Nasution ID, Hosoi M (1986b) Topographic representation of lower and upper teeth within the trigeminal sensory nuclei of adult cat as demonstrated by the transganglionic transport of horseradish peroxidase. J Comp Neurol 251:299–316.

Shigenaga Y, Yoshida A, Mitsuhiro Y, Doe K, Suemune S (1988a) Morphological and functional properties of trigeminal nucleus oralis neurons projecting to the trigeminal motor nucleus of the cat. Brain Res 416:143–149.

Shigenaga Y, Yoshida A, Tsuru K, Mitsuhiro Y, Otani K, Cao CQ (1988b) Physiological and morphological characteristics of cat masticatory motoneurons–intracellular injection of HRP. Brain Res 416:238–256.

Shigenaga Y, Doe K, Suemune S, Mitsuhiro Y, Tsuru K, Otani K, Shirana Y, Hosoi M, Yoshida A, Kagawa K (1989) Physiological and morphological characteristics of periodontal mesencephalic trigeminal neurons in the cat–intra-axonal staining with HRP. Brain Res 505:91–110.

Shigenaga Y, Mitsuhiro Y, Shirana Y, Tsuru H (1990) Two types of jaw-muscle spindle afferents in the cat as demonstrated by intra-axonal staining with HRP. Brain Res 514:219–237.

Shigenaga Y, Hirose Y, Yoshida A, Fukami H, Honma S, Bae YC (2000) Quantitative ultrastructure of physiologically identified premotoneuron terminals in the trigeminal motor nucleus in the cat. J Comp Neurol 426:13–30.

Somogyi P, Nunzi MG, Gorio A, Smith AD (1983) A new type of specific interneuron in the monkey hippocampus forming synapses exclusively with the axon initial segments of pyramidal cells. Brain Res 259:137–142.

Takemura M, Sugimoto T, Shigenaga Y (1991) Difference in central projection of primary afferents innervating facial and intraoral structures in the rat. Exp Neurol 111:324–331.

Tamás G, Buhl EH, Somogyi P (1997) Fast IPSPs elicited via multiple synaptic release sites by different types of GABAergic neurone in the cat visual cortex. J Physiol (Lond) 500:715–738.

Taylor A (1990) Proprioceptive control of jaw movement. In: Neurophysiology of the jaws and teeth (Taylor A, ed), pp 237–267. Hampshire, UK: Macmillan.

Thomson AM, West DC, Hahn J, Deuchars J (1996) Single axon IPSPs elicited in pyramidal cells by three classes of interneurons in slices of rat neocortex. J Physiol (Lond) 496:81–102.

Tsuru K, Otani K, Kajiyama K, Suemune S, Shigenaga Y (1989) Central terminations of periodontal mechanoreceptive and tooth pulp afferents in the trigeminal principal and oral nuclei of the cat. Brain Res 485:29–61.

Turman Jr JE, Chandler SH (1994) Immunohistochemical localization of glutamate and glutaminase in guinea pig trigeminal premotoneurons. Brain Res 634:49–61.

Westberg KG, Sandstrom G, Olsson KÅ (1995) Integration in trigeminal premotor interneurones in the cat. 3. Input characteristics and synaptic actions of neurones in subnucleus-γ of the oral nucleus of the spinal trigeminal tract with a projection to the masseteric motoneurone subnucleus. Exp Brain Res 104:449–461.

Yabuta NH, Yasuda K, Nagase Y, Yoshida A, Fukunishi Y, Shigenaga Y (1996) Light microscopic observation of the contacts made between two spindle afferent types and α-motoneurons in the cat trigeminal motor nucleus. J Comp Neurol 374:436–450.

Yoshida A, Yasuda K, Dostrovsky JO, Bae YC, Takemura M, Shigenaga Y, Sessle BJ (1994) Two major types of premotoneurons in the feline trigeminal nucleus oralis neurons as demonstrated by intracellular staining with HRP. J Comp Neurol 347:495–514.

Yoshida A, Hiraga T, Moritani M, Chen K, Takatsuki Y, Hirose Y, Bae YC, Shigenaga Y (1998) Morphologic characteristics of physiologically defined neurons in the cat trigeminal nucleus principalis. J Comp Neurol 401:308–328.

Yoshida A, Mukai N, Moritani M, Nagase Y, Hirose Y, Honma S, Fukami H, Takagi K, Matsuya T, Shigenaga Y (1999) Physiologic and morphologic properties of motoneurons and spindle afferents innervating the temporal muscles in the cat. J Comp Neurol 406:29–50.